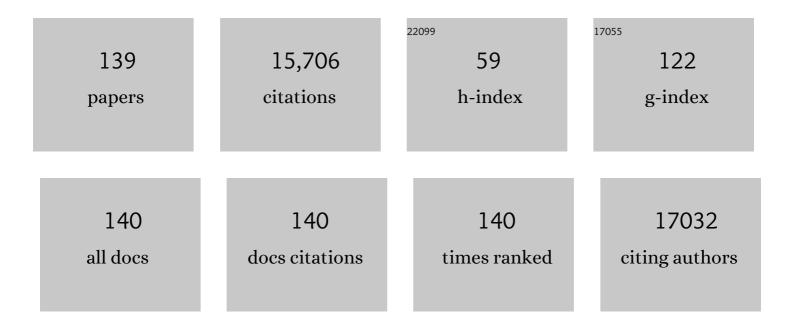


List of Publications by Year in descending order

Source: https://exaly.com/author-pdf/6071258/publications.pdf Version: 2024-02-01



#	Article	IF	CITATIONS
1	Cu nanowires shelled with NiFe layered double hydroxide nanosheets as bifunctional electrocatalysts for overall water splitting. Energy and Environmental Science, 2017, 10, 1820-1827.	15.6	1,002
2	Bismuth oxyhalide nanomaterials: layered structures meet photocatalysis. Nanoscale, 2014, 6, 8473-8488.	2.8	774
3	Non-noble metal-nitride based electrocatalysts for high-performance alkaline seawater electrolysis. Nature Communications, 2019, 10, 5106.	5.8	742
4	Giant Enhancement of Internal Electric Field Boosting Bulk Charge Separation for Photocatalysis. Advanced Materials, 2016, 28, 4059-4064.	11.1	538
5	Ultrafast room-temperature synthesis of porous S-doped Ni/Fe (oxy)hydroxide electrodes for oxygen evolution catalysis in seawater splitting. Energy and Environmental Science, 2020, 13, 3439-3446.	15.6	507
6	Water splitting by electrolysis at high current densities under 1.6 volts. Energy and Environmental Science, 2018, 11, 2858-2864.	15.6	438
7	Enhancement of photocatalytic activity of mesoporous TiO2 by using carbon nanotubes. Applied Catalysis A: General, 2005, 289, 186-196.	2.2	434
8	Superior visible light hydrogen evolution of Janus bilayer junctions via atomic-level charge flow steering. Nature Communications, 2016, 7, 11480.	5.8	403
9	Enhancement of adsorption and photocatalytic activity of TiO2 by using carbon nanotubes for the treatment of azo dye. Applied Catalysis B: Environmental, 2005, 61, 1-11.	10.8	377
10	Preparation of multi-walled carbon nanotube supported TiO2 and its photocatalytic activity in the reduction of CO2 with H2O. Carbon, 2007, 45, 717-721.	5.4	346
11	Highly efficient photocatalytic removal of sodium pentachlorophenate with Bi3O4Br under visible light. Applied Catalysis B: Environmental, 2013, 136-137, 112-121.	10.8	338
12	<mml:math xmlns:mml="http://www.w3.org/1998/Math/MathML"><mml:mrow><mml:msup><mml:mrow><mml:mtext>Ti< the Surface of Titanium Dioxide: Generation, Properties and Photocatalytic Application. Journal of Nanomaterials, 2012, 2012, 1-13.</mml:mtext></mml:mrow></mml:msup></mml:mrow></mml:math 	/mml:mtex 1.5	t> ج/mml:mrc ع20
13	A molecular-imprint nanosensor for ultrasensitive detection of proteins. Nature Nanotechnology, 2010, 5, 597-601.	15.6	322
14	A New View of Supercapacitors: Integrated Supercapacitors. Advanced Energy Materials, 2019, 9, 1901081.	10.2	315
15	Dropwise condensation on superhydrophobic surfaces with two-tier roughness. Applied Physics Letters, 2007, 90, 173108.	1.5	302
16	Hydrothermal preparation and visible-light photocatalytic activity of Bi2WO6 powders. Journal of Solid State Chemistry, 2005, 178, 1968-1972.	1.4	288
17	Single Fe Atom on Hierarchically Porous S, N odoped Nanocarbon Derived from Porphyra Enable Boosted Oxygen Catalysis for Rechargeable Znâ€Air Batteries. Small, 2019, 15, e1900307.	5.2	273
18	Adsorption of Water-Soluble Dye onto Functionalized Resin. Journal of Colloid and Interface Science, 2001, 242, 288-293.	5.0	270

#	Article	IF	CITATIONS
19	Visible-Light-Driven Photocatalytic Inactivation of <i>E. coli</i> K-12 by Bismuth Vanadate Nanotubes: Bactericidal Performance and Mechanism. Environmental Science & Technology, 2012, 46, 4599-4606.	4.6	254
20	Hierarchical Cu@CoFe layered double hydroxide core-shell nanoarchitectures as bifunctional electrocatalysts for efficient overall water splitting. Nano Energy, 2017, 41, 327-336.	8.2	252
21	Atypical Oxygen-Bearing Copper Boosts Ethylene Selectivity toward Electrocatalytic CO ₂ Reduction. Journal of the American Chemical Society, 2020, 142, 11417-11427.	6.6	250
22	In Situ Fenton Reagent Generated from TiO ₂ /Cu ₂ O Composite Film:  a New Way to Utilize TiO ₂ under Visible Light Irradiation. Environmental Science & Technology, 2007, 41, 6264-6269.	4.6	227
23	Ternary Ni2(1-x)Mo2xP nanowire arrays toward efficient and stable hydrogen evolution electrocatalysis under large-current-density. Nano Energy, 2018, 53, 492-500.	8.2	216
24	Recent developments in earth-abundant and non-noble electrocatalysts for water electrolysis. Materials Today Physics, 2018, 7, 121-138.	2.9	203
25	Enhanced Activity and Stability of Carbon-Decorated Cuprous Oxide Mesoporous Nanorods for CO ₂ Reduction in Artificial Photosynthesis. ACS Catalysis, 2016, 6, 6444-6454.	5.5	201
26	Synthesis and internal electric field dependent photoreactivity of Bi ₃ O ₄ Cl single-crystalline nanosheets with high {001} facet exposure percentages. Nanoscale, 2014, 6, 167-171.	2.8	185
27	Mechanistic Study of Codoped Titania with Nonmetal and Metal Ions: A Case of C + Mo Codoped TiO ₂ . ACS Catalysis, 2012, 2, 391-398.	5.5	171
28	Defective and ultrathin NiFe LDH nanosheets decorated on V-doped Ni ₃ S ₂ nanorod arrays: a 3D core–shell electrocatalyst for efficient water oxidation. Journal of Materials Chemistry A, 2019, 7, 18118-18125.	5.2	171
29	Amorphous NiFe layered double hydroxide nanosheets decorated on 3D nickel phosphide nanoarrays: a hierarchical core–shell electrocatalyst for efficient oxygen evolution. Journal of Materials Chemistry A, 2018, 6, 13619-13623.	5.2	169
30	N-doped Ni-Mo based sulfides for high-efficiency and stable hydrogen evolution reaction. Applied Catalysis B: Environmental, 2020, 276, 119137.	10.8	150
31	Facetâ€Level Mechanistic Insights into General Homogeneous Carbon Doping for Enhanced Solarâ€ŧoâ€Hydrogen Conversion. Advanced Functional Materials, 2015, 25, 2189-2201.	7.8	146
32	Adsorption of water-soluble dyes onto modified resin. Chemosphere, 2004, 54, 425-430.	4.2	142
33	Facile Synthesis of Flowerlike Cu2O Nanoarchitectures by a Solution Phase Route. Crystal Growth and Design, 2007, 7, 87-92.	1.4	139
34	Photocatalytic reduction of CO2 to CO over copper decorated g-C3N4 nanosheets with enhanced yield and selectivity. Applied Surface Science, 2018, 427, 1165-1173.	3.1	136
35	In Situ Polymerized PAN-Assisted S/C Nanosphere with Enhanced High-Power Performance as Cathode for Lithium/Sulfur Batteries. Nano Letters, 2015, 15, 5116-5123.	4.5	128
36	Zn-Doped CdS Nanoarchitectures Prepared by Hydrothermal Synthesis: Mechanism for Enhanced Photocatalytic Activity and Stability under Visible Light. Journal of Physical Chemistry C, 2012, 116, 9078-9084.	1.5	120

#	Article	IF	CITATIONS
37	Visible-light driven CO2 reduction coupled with water oxidation on Cl-doped Cu2O nanorods. Nano Energy, 2019, 60, 576-582.	8.2	115
38	A universal synthesis strategy to make metal nitride electrocatalysts for hydrogen evolution reaction. Journal of Materials Chemistry A, 2019, 7, 19728-19732.	5.2	114
39	One-dimensional shape-controlled preparation of porous Cu2O nano-whiskers by using CTAB as a template. Journal of Solid State Chemistry, 2004, 177, 4640-4647.	1.4	109
40	Octahedral Cu2O-modified TiO2 nanotube arrays for efficient photocatalytic reduction of CO2. Chinese Journal of Catalysis, 2015, 36, 2229-2236.	6.9	105
41	Template-free synthesis of BiVO ₄ nanostructures: I. Nanotubes with hexagonal cross sections by oriented attachment and their photocatalytic property for water splitting under visible light. Nanotechnology, 2009, 20, 115603.	1.3	103
42	p-Type and n-type Cu2O semiconductor thin films: Controllable preparation by simple solvothermal method and photoelectrochemical properties. Electrochimica Acta, 2011, 56, 2735-2739.	2.6	98
43	Ultrafast fabrication of porous transition metal foams for efficient electrocatalytic water splitting. Applied Catalysis B: Environmental, 2021, 288, 120002.	10.8	98
44	Preparation of Fenton reagent with H2O2 generated by solar light-illuminated nano-Cu2O/MWNTs composites. Applied Catalysis A: General, 2006, 299, 292-297.	2.2	95
45	Preparation, characterization and photocatalytic properties of ZnO-coated multi-walled carbon nanotubes. Materials Science and Engineering B: Solid-State Materials for Advanced Technology, 2009, 163, 194-198.	1.7	93
46	Preparation, characterization and photocatalytic properties of CdS nanoparticles dotted on the surface of carbon nanotubes. Nanotechnology, 2008, 19, 115709.	1.3	90
47	Copper nanoparticle interspersed MoS ₂ nanoflowers with enhanced efficiency for CO ₂ electrochemical reduction to fuel. Dalton Transactions, 2017, 46, 10569-10577.	1.6	81
48	VS ₄ with a chain crystal structure used as an intercalation cathode for aqueous Zn-ion batteries. Journal of Materials Chemistry A, 2020, 8, 10761-10766.	5.2	77
49	Fe induced nanostructure reorganization and electronic structure modulation over CoNi (oxy)hydroxide nanorod arrays for boosting oxygen evolution reaction. Chemical Engineering Journal, 2021, 403, 126304.	6.6	75
50	Enhanced photocatalytic activity and stability of semiconductor by Ag doping and simultaneous deposition: the case of CdS. RSC Advances, 2013, 3, 20782.	1.7	73
51	Facile in situ fabrication of Cu2O@Cu metal-semiconductor heterostructured nanorods for efficient visible-light driven CO2 reduction. Chemical Engineering Journal, 2020, 385, 123940.	6.6	71
52	Three-dimensional interconnected core–shell networks with Ni(Fe)OOH and M–N–C active species together as high-efficiency oxygen catalysts for rechargeable Zn–air batteries. Journal of Materials Chemistry A, 2019, 7, 19045-19059.	5.2	70
53	A robust 2D organic polysulfane nanosheet with grafted polycyclic sulfur for highly reversible and durable lithium-organosulfur batteries. Nano Energy, 2019, 57, 635-643.	8.2	69
54	New Way for CO ₂ Reduction under Visible Light by a Combination of a Cu Electrode and Semiconductor Thin Film: Cu ₂ O Conduction Type and Morphology Effect. Journal of Physical Chemistry C, 2014, 118, 24467-24478.	1.5	68

#	Article	IF	CITATIONS
55	TiO2 Nanotube Arrays Grafted with MnO2 Nanosheets as High-Performance Anode for Lithium Ion Battery. Electrochimica Acta, 2015, 156, 252-260.	2.6	68
56	Cu ₂ O Homojunction Solar Cells: F-Doped N-type Thin Film and Highly Improved Efficiency. Journal of Physical Chemistry C, 2015, 119, 22803-22811.	1.5	68
57	Template-free synthesis of BiVO ₄ nanostructures: II. Relationship between various microstructures for monoclinic BiVO ₄ and their photocatalytic activity for the degradation of rhodamine B under visible light. Nanotechnology, 2009, 20, 405602.	1.3	64
58	Bifunctional photocatalysis of TiO2/Cu2O composite under visible light: Ti3+ in organic pollutant degradation and water splitting. Journal of Physics and Chemistry of Solids, 2011, 72, 1104-1109.	1.9	64
59	Self-assembled Cu2O flowerlike architecture: Polyol synthesis, photocatalytic activity and stability under simulated solar light. Materials Research Bulletin, 2010, 45, 961-968.	2.7	63
60	CuBi2O4 single crystal nanorods prepared by hydrothermal method: Growth mechanism and optical properties. Materials Research Bulletin, 2011, 46, 1443-1450.	2.7	62
61	Dynamic Restructuring of Coordinatively Unsaturated Copper Paddle Wheel Clusters to Boost Electrochemical CO ₂ Reduction to Hydrocarbons**. Angewandte Chemie - International Edition, 2022, 61, .	7.2	61
62	Synergistic effect of adsorption and visible-light photocatalysis for organic pollutant removal over BiVO4/carbon sphere nanocomposites. Applied Surface Science, 2018, 453, 394-404.	3.1	60
63	Sonication assisted deposition of Cu2O nanoparticles on multiwall carbon nanotubes with polyol process. Carbon, 2005, 43, 670-673.	5.4	58
64	Synthesis of novel high-voltage cathode material LiCoPO4 via rheological phase method. Journal of Alloys and Compounds, 2010, 502, 407-410.	2.8	58
65	Nitrogen-doped TiO2 nanoparticles by using EDTA as nitrogen source and soft template: Simple preparation, mesoporous structure, and photocatalytic activity under visible light. Journal of Alloys and Compounds, 2012, 540, 228-235.	2.8	58
66	Aligned 2-D Nanosheet Cu2O Film: Oriented Deposition on Cu Foil and Its Photoelectrochemical Property. Journal of Physical Chemistry C, 2008, 112, 18916-18922.	1.5	57
67	Robust and selective electrochemical reduction of CO ₂ : the case of integrated 3D TiO ₂ @MoS ₂ architectures and Ti–S bonding effects. Journal of Materials Chemistry A, 2018, 6, 4706-4713.	5.2	56
68	Realizing a Rechargeable Highâ€Performance Cu–Zn Battery by Adjusting the Solubility of Cu ²⁺ . Advanced Functional Materials, 2019, 29, 1905979.	7.8	54
69	Coating MWNTs with Cu2O of different morphology by a polyol process. Journal of Solid State Chemistry, 2005, 178, 1488-1494.	1.4	53
70	Hierarchical 3D TiO ₂ @Fe ₂ O ₃ nanoframework arrays as high-performance anode materials. Nanoscale, 2014, 6, 6463-6467.	2.8	53
71	Combination study of DFT calculation and experiment for photocatalytic properties of S-doped anatase TiO2. Applied Surface Science, 2014, 319, 50-59.	3.1	51
72	High-performance seawater oxidation by a homogeneous multimetallic layered double hydroxide electrocatalyst. Proceedings of the National Academy of Sciences of the United States of America, 2022, 119, e2202382119.	3.3	51

#	Article	IF	CITATIONS
73	Controllable synthesis of self-assembled Cu2S nanostructures through a template-free polyol process for the degradation of organic pollutant under visible light. Materials Research Bulletin, 2009, 44, 1834-1841.	2.7	50
74	Facile Synthesis of Carbon Spheres with Uniformly Dispersed MnO Nanoparticles for Lithium Ion Battery Anode. Electrochimica Acta, 2015, 152, 44-52.	2.6	49
75	Synthesis of (CuIn)xCd2(1â~'x)S2 photocatalysts for H2 evolution under visible light by using a low-temperature hydrothermal method. International Journal of Hydrogen Energy, 2010, 35, 3297-3305.	3.8	45
76	Ultraporous interweaving electrospun microfibers from PCL–PEO binary blends and their inflammatory responses. Nanoscale, 2014, 6, 3392.	2.8	45
77	Nitrogen-coordinated metallic cobalt disulfide self-encapsulated in graphitic carbon for electrochemical water oxidation. Applied Catalysis B: Environmental, 2020, 268, 118449.	10.8	44
78	Stable core–shell ZIF-8@ZIF-67 MOFs photocatalyst for highly efficient degradation of organic pollutant and hydrogen evolution. Journal of Materials Research, 2021, 36, 602-614.	1.2	44
79	Electrolyzer with hierarchical transition metal sulfide and phosphide towards overall water splitting. Materials Today Physics, 2019, 11, 100162.	2.9	43
80	A robust bifunctional catalyst for rechargeable Zn-air batteries: Ultrathin NiFe-LDH nanowalls vertically anchored on soybean-derived Fe-N-C matrix. Nano Research, 2021, 14, 1175-1186.	5.8	43
81	Synthesis of Bi2O3/Cu2O nanoflowers by hydrothermal method and its photocatalytic activity enhancement under simulated sunlight. Journal of Alloys and Compounds, 2013, 560, 132-141.	2.8	42
82	Design of a unique 3D-nanostructure to make MnO2 work as supercapacitor material in acid environment. Chemical Engineering Journal, 2017, 321, 554-563.	6.6	42
83	Nano-sized Li4Ti5O12 anode material with excellent performance prepared by solid state reaction: The effect of precursor size and morphology. Electrochimica Acta, 2013, 112, 356-363.	2.6	41
84	Carbon-decorated Li ₄ Ti ₅ O ₁₂ /rutile TiO ₂ mesoporous microspheres with nanostructures as high-performance anode materials in lithium-ion batteries. Nanotechnology, 2014, 25, 175402.	1.3	39
85	Adsorption of Water-Soluble Dyes onto Resin NKZ. Industrial & Engineering Chemistry Research, 2003, 42, 6898-6903.	1.8	38
86	Visible-light Energy Storage by Ti3+ in TiO2/Cu2O Bilayer Film. Chemistry Letters, 2009, 38, 1154-1155.	0.7	38
87	Neodymium-Doped <mml:math xmlns:mml="http://www.w3.org/1998/Math/MathML"><mml:msub><mml:mrow><mml:mtext>TiO</mml:mtext> Anatase and Brookite Two Phases: Mechanism for Photocatalytic Activity Enhancement under Visible Light and the Role of Electron. International Journal of Photoenergy. 2012. 2012. 1-10.</mml:mrow></mml:msub></mml:math 	<td>ows<mml:m< td=""></mml:m<></td>	ows <mml:m< td=""></mml:m<>
88	Enhanced photocatalytic activity and stability of interstitial Ga-doped CdS: Combination of experiment and calculation. Catalysis Today, 2014, 224, 104-113.	2.2	38
89	Cu2O nanorod thin films prepared by CBD method with CTAB: Substrate effect, deposition mechanism and photoelectrochemical properties. Materials Chemistry and Physics, 2011, 127, 433-439.	2.0	37
90	TiO2 mesoporous microspheres with nanorod structure: facile synthesis and superior electrochemical performance. Electrochimica Acta, 2014, 120, 231-239.	2.6	37

#	Article	IF	CITATIONS
91	Design of SnO ₂ /C hybrid triple-layer nanospheres as Li-ion battery anodes with high stability and rate capability. Journal of Materials Chemistry A, 2015, 3, 2748-2755.	5.2	37
92	Nickel phosphide based hydrogen producing catalyst with low overpotential and stability at high current density. Electrochimica Acta, 2019, 299, 756-761.	2.6	36
93	Roles of heteroatoms in electrocatalysts for alkaline water splitting: A review focusing on the reaction mechanism. Chinese Journal of Catalysis, 2022, 43, 2091-2110.	6.9	36
94	Reaction mechanisms for reduction of CO2 to CO on monolayer MoS2. Applied Surface Science, 2020, 499, 143964.	3.1	35
95	Sand flower layered double hydroxides synthesized by co-precipitation for CO2 capture: Morphology evolution mechanism, agitation effect and stability. Materials Chemistry and Physics, 2013, 140, 159-167.	2.0	34
96	TiO2 nanoparticles with high ability for selective adsorption and photodegradation of textile dyes under visible light by feasible preparation. Journal of Physics and Chemistry of Solids, 2014, 75, 86-93.	1.9	34
97	N-type Cu2O Film for Photocatalytic and Photoelectrocatalytic Processes: Its stability and Inactivation of E. coli. Electrochimica Acta, 2015, 153, 583-593.	2.6	34
98	TiO 2 thin films with rutile phase prepared by DC magnetron co-sputtering at room temperature: Effect of Cu incorporation. Applied Surface Science, 2015, 345, 49-56.	3.1	32
99	Nest-like V ₃ O ₇ self-assembled by porous nanowires as an anode supercapacitor material and its performance optimization through bonding with N-doped carbon. Journal of Materials Chemistry A, 2018, 6, 16475-16484.	5.2	32
100	Hierarchical porous Fe2O3 assisted with graphene-like carbon as high-performance lithium battery anodes. Materials Today Physics, 2017, 3, 7-15.	2.9	30
101	Self-supported ultrathin bismuth nanosheets acquired by <i>in situ</i> topotactic transformation of BiOCl as a high performance aqueous anode material. Journal of Materials Chemistry A, 2019, 7, 6784-6792.	5.2	29
102	Electrochemistry and electrocatalysis of myoglobin on carbon coated Fe3O4 nanospindle modified carbon ionic liquid electrode. RSC Advances, 2012, 2, 5676.	1.7	27
103	Co-dopant influence on near-infrared luminescence properties of Zn 2 SnO 4 :Cr 3+ , Eu 3+ ceramic discs. Journal of Alloys and Compounds, 2016, 686, 407-412.	2.8	27
104	Design of multidimensional nanocomposite material to realize the application both in energy storage and electrocatalysis. Science Bulletin, 2018, 63, 152-154.	4.3	27
105	Unraveling the Role of Nitrogenâ€Doped Carbon Nanowires Incorporated with <scp>MnO₂</scp> Nanosheets as High Performance Cathode for Zincâ€Ion Batteries. Energy and Environmental Materials, 2023, 6, .	7.3	27
106	Photocatalytic activity enhancement of CdS through In doping by simple hydrothermal method. Journal of Physics and Chemistry of Solids, 2013, 74, 647-652.	1.9	26
107	A Model to Stabilize CO ₂ Uptake Capacity during Carbonation–Calcination Cycles and its Case of CaO–MgO. Environmental Science & Technology, 2017, 51, 552-559.	4.6	26
108	Effect of Dye Structure on the Interaction between Organic Flocculant PAN-DCD and Dye. Industrial & Engineering Chemistry Research, 2002, 41, 1589-1596.	1.8	25

#	Article	IF	CITATIONS
109	Enhanced photocatalytic activity of α-Bi2O3 with high electron-hole mobility by codoping approach: A first-principles study. Applied Surface Science, 2015, 358, 449-456.	3.1	25
110	Ultraporous nanofeatured PCL–PEO microfibrous scaffolds enhance cell infiltration, colonization and myofibroblastic differentiation. Nanoscale, 2015, 7, 14989-14995.	2.8	25
111	Platinum nanoparticles supported on defective tungsten bronze-type KSr ₂ Nb ₅ O ₁₅ as a novel photocatalyst for efficient ethylene oxidation. Journal of Materials Chemistry A, 2017, 5, 18998-19006.	5.2	25
112	Application of flower-like SnS ₂ nanoparticles for direct electrochemistry of hemoglobin and its electrocatalysis. Analytical Methods, 2014, 6, 404-409.	1.3	23
113	Fermi-level-tuned MOF-derived N-ZnO@NC for photocatalysis: A key role of pyridine-N-Zn bond. Journal of Materials Science and Technology, 2022, 112, 68-76.	5.6	23
114	Electronic Structure Regulation of Nickel Phosphide for Efficient Overall Water Splitting. Inorganic Chemistry, 2022, 61, 9318-9327.	1.9	23
115	Carbon-Infused MoS2 Supported on TiO2 Nanosheet Arrays for Intensified Anodes in Lithium Ion Batteries. Electrochimica Acta, 2016, 212, 59-67.	2.6	21
116	H ₂ O ₂ Treated CdS with Enhanced Activity and Improved Stability by a Weak Negative Bias for CO ₂ Photoelectrocatalytic Reduction. ACS Sustainable Chemistry and Engineering, 2019, 7, 4325-4334.	3.2	21
117	Facile preparation of W5O14 nanosheet arrays with large crystal channels as high-performance negative electrode for supercapacitor. Electrochimica Acta, 2020, 330, 135209.	2.6	20
118	Experimental method to explore the adaptation degree of type-II and all-solid-state Z-scheme heterojunction structures in the same degradation system. Chinese Journal of Catalysis, 2020, 41, 1522-1534.	6.9	20
119	Role of oxygen in copper-based catalysts for carbon dioxide electrochemical reduction. Materials Today Physics, 2021, 20, 100443.	2.9	19
120	Hydrogen plasma reduced potassium titanate as a high power and ultralong lifespan anode material for sodium-ion batteries. Journal of Materials Chemistry A, 2018, 6, 22037-22042.	5.2	18
121	Magnetic Properties of Cu _{<i>m</i>} O _{<i>n</i>} Clusters: A First Principles Study. Journal of Physical Chemistry A, 2010, 114, 8417-8422.	1.1	17
122	Characterization and high pollutant removal ability of buoyant (C, N)–TiO ₂ /PTFE flakes prepared by high-energy ball-milling. RSC Advances, 2014, 4, 40019.	1.7	17
123	Delivery of dexamethasone from electrospun PCL–PEO binary fibers and their effects on inflammation regulation. RSC Advances, 2015, 5, 34166-34172.	1.7	17
124	Nd3+ ions induced rational morphology control of transition metal oxides for high energy storage performance. Journal of Power Sources, 2020, 472, 228599.	4.0	16
125	High spatially resolved morphological, structural and spectroscopical studies on copper oxide nanocrystals. Nanotechnology, 2007, 18, 075705.	1.3	15
126	Interconnected mesoporous NiO sheets deposited onto TiO ₂ nanosheet arrays as binder-free anode materials with enhanced performance for lithium ion batteries. RSC Advances, 2015, 5, 101247-101256.	1.7	15

#	Article	IF	CITATIONS
127	Visible-light responsive boron and nitrogen codoped anatase TiO2 with exposed {0 0 1} facet: Calculation and experiment. Applied Surface Science, 2019, 466, 568-577.	3.1	15
128	Assembly of multi-functional nanocomponents on periodic nanotube array for biosensors. Micro and Nano Letters, 2009, 4, 27-33.	0.6	14
129	LSDA+ U study on the electronic and anti-ferromagnetic properties of Ni-doped CuO and Cu-doped NiO. Chinese Journal of Catalysis, 2017, 38, 767-773.	6.9	14
130	Interactions between organic flocculant PAN–DCD and dyes. Chemosphere, 2001, 44, 1287-1292.	4.2	13
131	Energy Storage in Bifunctional TiO2 Composite Materials under UV and Visible Light. Energies, 2009, 2, 1009-1030.	1.6	13
132	A simplified chemical synthesis of Cu2O films with periodic pattern transfer. Thin Solid Films, 2010, 518, 6738-6745.	0.8	10
133	A novel H2O2-assisted method to fabricate Li4Ti5O12/TiO2 materials for high-performance energy storage. Electrochimica Acta, 2018, 281, 142-151.	2.6	10
134	Ultrafast charge in Zn-based batteries through high-potential deposition. Materials Today Physics, 2021, 19, 100425.	2.9	9
135	Multiple magnification effects of Ce^3+ ions on near-infrared persistent luminescence of Cr-doped LaAlO_3. Optical Materials Express, 2016, 6, 922.	1.6	8
136	Synthesis and Characteristic of Cuprous Oxide Nano-Whiskers with Photocatalytic Activity under Visible Light. Materials Science Forum, 2005, 475-479, 3531-3534.	0.3	5
137	Ultra-small Ni(HCO ₃) ₂ as a water dissociation promoter boosting the alkaline hydrogen electrocatalysis performance of MoS ₂ . Chemical Communications, 2020, 56, 12065-12068.	2.2	5
138	Cu2O nanorods with large surface area for photodegradation of organic pollutant under visible light. , 2007, , .		2
139	Comparative study of oxidative stress induced by sand flower and schistose nanosized layered double hydroxides in N2a cells. Frontiers in Biology, 2015, 10, 279-286.	0.7	2